Nuclear Instruments and Methods in Physics Research B 348 (2015) 23–28

Contents lists available at ScienceDirect

Nuclear Instruments and Methods in Physics Research B

journal homepage: www.elsevier.com/locate/nimb

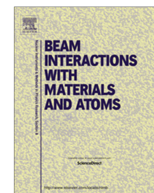

Development of ion sources: Towards high brightness for proton beam writing applications

Nannan Liu [a], P. Santhana Raman [a], Xinxin Xu [a], Huei Ming Tan [b], Anjam Khursheed [b], Jeroen A. van Kan [a,*]

[a] Centre for Ion Beam Applications, Department of Physics, National University of Singapore, Singapore 117542, Singapore
[b] ESP, ECE, National University of Singapore, Singapore 117583, Singapore

ARTICLE INFO

Article history:
Received 25 July 2014
Received in revised form 22 December 2014
Accepted 12 January 2015
Available online 6 February 2015

Keywords:
Proton beam writing
Ion source
Ion source reduced brightness

ABSTRACT

An Ion Source Test Bench (ISTB) has been designed and commissioned to facilitate the measurement of ion beam reduced brightness (B_r) obtained from different ion sources. Preliminary B_r measurements were carried out, with RF ion source, in the ISTB for He ions. Meanwhile we have also fabricated and tested a novel ion source called electron impact gas ion source, whose reduced brightness is expected to reach up to 10^7 pA/μm^2 mrad^2 MeV. Initial ion-current measurements from such electron impact gas ion source (tested inside an environmental SEM) has yielded about 300 pA of Ar ions. The areal ion current density from this electron impact gas ion source is found to be at least 380 times higher than the existing RF ion source. This novel ion source is promising for application in proton beam writing lithography with feature sizes smaller than 10 nm.

© 2015 Elsevier B.V. All rights reserved.

1. Introduction

In the recent past we have demonstrated the potential of proton beam writing (PBW) as a leading candidate for the next generation lithography technique [1–3], highlighted in the Japanese government's Nanotechnology Business Creation Initiative (NBCI) roadmap 2010 [4]. We are now progressing towards sub-10 nm lithography in nuclear microprobe experiments [5,6]. To achieve this goal, plans are being rolled out to improve the performance of the existing low brightness radio frequency (RF) ion source, used for the production of proton beams at Centre for Ion Beam Applications (CIBA), National University of Singapore (NUS). This RF ion source has potential to deliver higher brightness [7]. An Ion Source Test Bench (ISTB) set-up has been designed and commissioned in-house to extract the full potential of the existing RF ion source by improving its reduced brightness, as attempted by a few other researchers [8–12]. First brightness measurements obtained from RF ion source in this ISTB will be presented in this paper. In future the ISTB will be used to test novel high brightness ion source designs, which has the capability to form part of a compact PBW system.

In search of high brightness ion sources, we are developing a modified electron impact gas ion source, based on the design by the Charged Particle Optics group, Delft University of Technology. Their electron impact gas ion source is expected to have smaller virtual source size (∼100 nm) and deliver higher reduced brightness, B_r (∼10^7 pA/μm^2 mrad^2 MeV for Ar^+ beam) [13]. Prototypes of the miniaturized gas ionization chambers have been fabricated in CIBA, NUS. First experiments with a small gas ionization chamber were performed inside a field emission Scanning Electron Microscope (SEM) in NUS. The design of the current ionization chamber is equipped to admit different gases (e.g. helium, argon, and hydrogen) into the ion source. This paper presents preliminary results about the extracted ion currents (for air and argon) from this ion source.

2. Experimental procedures

2.1. Ion Source Test Bench (ISTB) set-up

Fig. 1 shows the schematic diagram of the ISTB set-up. The current version of ISTB is coupled with a RF ion source. An oscillating RF voltage (∼100 MHz) is capacitively coupled onto a quartz tube, which is filled with the gas of interest, that produces a stable plasma. The positively biased plasma is then extracted through a 2 mm diameter canal, with a variable extraction voltage of 0 to −3 kV. The extracted beam is accelerated by passing through an acceleration column, which consists of an array of metal electrodes (separated by insulators) acting as a potential divider across the high voltage to the ground terminal. The accelerated beam is collimated using a Ni object aperture before entering a Wien filter

* Corresponding author.
E-mail address: phyjavk@nus.edu.sg (J.A. van Kan).

http://dx.doi.org/10.1016/j.nimb.2015.01.017
0168-583X/© 2015 Elsevier B.V. All rights reserved.

assembly, where ions of selected mass and charge state are transmitted un-deflected. The beam of interest will then pass through a Ni collimator aperture before reaching the target. The aperture assemblies will be used, in combination with the ion current measurements carried out on the target (where secondary electron suppression is taken care), to evaluate the reduced brightness of the ion beam (B_r).

2.2. The electron impact gas ion source concept

As mentioned early, we are developing a high brightness electron impact gas ion source, which will eventually be coupled to the ISTB. The idea of the electron impact gas ion source is to introduce an electron beam into a gas chamber through a small double aperture (100 nm to 1 μm diameter) as shown in Fig. 2. The gas chamber is miniaturized to provide a small spacing between two apertures (100 nm–1 μm). Once ions are produced inside the gas chamber by electron impact, they can be extracted through the double aperture by applying an electric field up to 10^6 V/m across the double aperture and followed by an extractor. The DC bias electric field (as shown in Fig. 2) corresponds to a small bias voltage of 1–9 V for the present system. Depending on the position where the ionization occurs along this electric field axis, the ions may have different initial energy (ranging from 1 to 9 eV) which translates to the ion source energy spread.

2.3. Fabrication of the ion source chamber

In the miniature gas chamber by Delft, two 100 nm thick alloy metal layers were used as the double aperture membranes and two 100 nm thick silicon nitride layers were bonded as spacer [13]. The fabrication of our modified ion source chamber, carried out in CIBA, NUS, was based on bonding two 1 μm thick silicon nitride membranes (supported by 530 μm thick Si) together (Fig. 3), with a 200 nm Ti layer as spacer.

Free-standing silicon nitride windows (300 × 300 μm and 50 × 50 μm) were created on the top chip (as shown in Fig. 3), using a sequential procedure of photolithography, reactive ion etching (for removal of top Si_3N_4 layer) followed by potassium hydroxide solution etching (for removal of Si layer). A reservoir (of dimension 6 mm × 1 mm × 200 nm), to hold the gas, was created at the interface between top and bottom chip. This is achieved by 200 nm Ti metal lift off, which serves as a spacer. A thin Cr + Au metal layer (<20 nm) was deposited at the chip's top and bottom sides for applying a bias voltage across the chip. The two chips were then glued together at the edges. An opening of about 20 × 20 μm on the free standing Si_3N_4 of the top chip (for gas inlet) and another opening of about 1.5 μm (for double aperture, as shown in Fig. 4) were created by focused ion beam milling (FEI Quanta Dual Beam), with a 30 keV Gallium ion beam current of 1–2 nA.

2.4. The electron impact gas ion source current measurement setup inside a SEM

The experimental ion source test setup was established inside a Schottky emission SEM (Philips XL30) system in NUS (Fig. 5). The SEM provides an electron beam with 300 eV to 1 keV beam energy and an injecting electron beam current up to 30 nA. The gas inlet pressure can be varied from 1 mbar to 2 bar, using a gas regulating valve. The bias voltage across the double aperture can be applied up to 9 V. An ion-extraction voltage, ranging between −1 and −5 kV, was applied onto the extractor plate (having 1 mm diameter opening) for an injection of 1 keV electron beam. This extractor plate is placed at the mid-point, with a spacing of 1.5 mm, between the double aperture (above) and Faraday cup (below). The extracted ion current is collected and measured using a Faraday cup (biased at −30 V). The extraction voltage was always set to a higher negative value than the incident electron beam acceleration voltage, to prevent the incident electrons from reaching the Faraday cup. Moreover this negative potential also effectively suppresses the secondary electron emission from the Faraday cup. This secondary electron suppression is confirmed by simulation using Lorentz software [14]. Lorentz simulation also predicts that, for ions exiting the 1 μm diameter double aperture, their trajectories have a lateral spread within 100 μm when passing through the extraction plane. Therefore all ions reach the Faraday cup.

3. Results and discussion

3.1. B_r measurement of the RF ion source in the ISTB

After a few trial experiments in the ISTB, the RF ion source produces He^+, N^+ and Ar^+ ions with different energies varying from 1 to 15 keV, yielding a maximum ion current of about 20–25 μA at the exit of the accelerating column. Here we will describe the results, and brightness measurements obtained with 1 keV He^+ ions.

It is to be noted that, since most of the ion source components and its power supplies were at high voltage terminal, they need to be operated remotely. This is achieved in our ISTB using a wireless communication system, which was developed in-house using National Instruments (NI) Compact Real-Time Input/Output (cRIO) hardware. This reconfigurable embedded control and acquisition

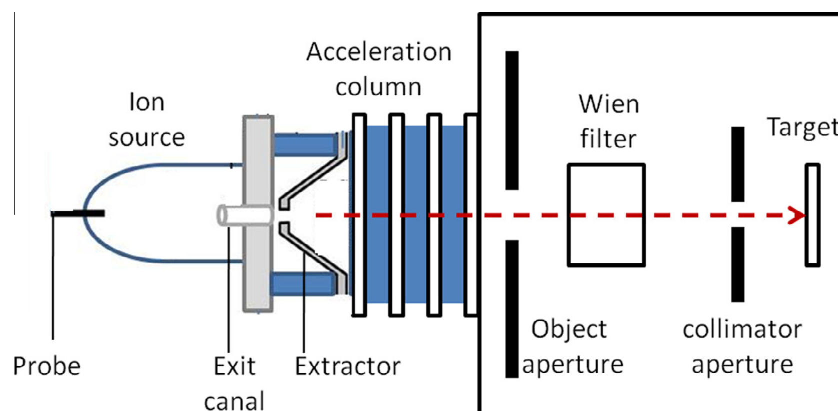

Fig. 1. Schematic of Ion Source Test Bench set-up, with a few ion beam diagnostics components. Dotted arrow represents the ion beam trajectory.

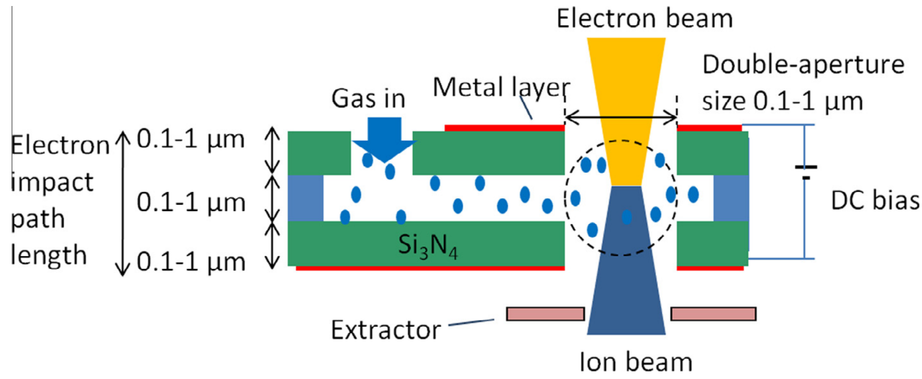

Fig. 2. Schematic of electron impact gas ion source. Electrons are focused into an ionization chamber filled with gas. Ions generated along the electron impact path length are accelerated by the applied DC bias between the double aperture and then extracted.

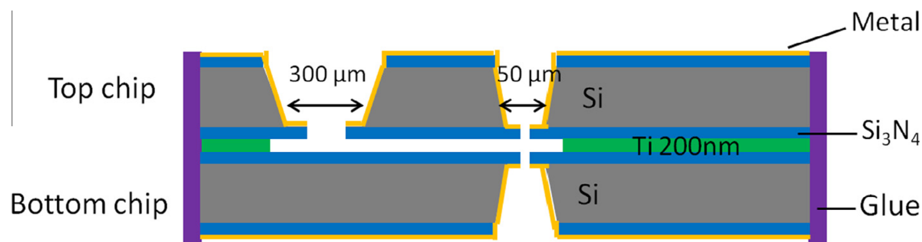

Fig. 3. Schematic design of the gas ionization chamber used in the electron impact gas ion source.

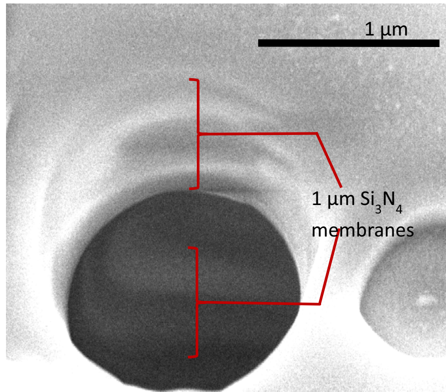

Fig. 4. SEM image of the double aperture with ~1.5 μm diameter and ~600 nm spacing.

system is controlled via a LabView VI program by a host PC at ground terminal.

The following experiment is to quantify the performance of the home-built Wien filter, which has been installed in the ISTB: used to analyze and spatially separate the incoming ions with different energies. Positive He ions, extracted from the ion source, pass through the acceleration column to acquire energies of 5 keV for He^+ and 10 keV for He^{2+} ions. We have measured a total He ion current of about 22 μA at the end of the acceleration column. The beam was collimated using a Ni object aperture (0.5 mm diameter). The collimated beam then enters the Wien filter assembly, where perpendicular magnetic field of 28.2 ± 10% mT and electric field of about 20 kV/m was maintained. SIMION 3D [15] simulation predicts a spatial separation of about 8.1 mm between He^+ (5 keV) and He^{2+} (10 keV) ions, closely matching the present experiment where a separation of about 8.8 mm on the target was observed. With a Ni collimator aperture (0.5 mm diameter) mounted on a translation arm above the target, the separated He^+ and He^{2+} ion beams were captured by this collimator aperture and the ion beam currents reaching the target were measured separately. The secondary electrons from the target were effectively suppressed by biasing the sample to about +9 V, during ion current measurement on the target. We have noticed a reduction, of the measured ion beam current, of about 45–50% between unbiased and biased target, and no further change was observed for any bias voltage above +9 V.

In another experiment, with the above ion current measurements, we have computed the reduced ion brightness for 1 keV He^+ ions from ISTB. Generally the B_r is measured using a formula, $B_r = \frac{I}{A_o\left(\frac{A_c}{D^2}\right)E}$ pA/μm² mrad² MeV , where I is the ion current in pA (here for He^+ = 300 pA), A_o is the area of the object aperture (in μm²), A_c is the area of the collimator aperture (in mm²), D is the distance between the object and collimator aperture in m (0.45 m) and E is the energy of the beam in MeV (0.001 MeV of He^+). A reduced brightness of about 1.60 pA/μm² mrad² MeV for He^+ ion beam has been achieved with beam half divergence of 1 mrad. Though the measured B_r seems to be comparatively lower than the highest reported value [8], the key difference here is that our value was obtained with a larger half divergence of 1 mrad. Thus our system is capable of delivering a bright beam, comparable to the B_r obtained at 0.1 mrad half divergence by Szymanski, and Jamieson [8], but with an order of magnitude larger beam half divergence. This allows higher beam current on the target due to wider collimator opening. The present B_r can be further improved with smaller beam half divergence, as reported in [8]. We are currently upgrading the ISTB system by installing variable object and collimator apertures with smaller opening sizes. This study will establish the effect of beam half divergence on the B_r, thereby hoping to increase the present B_r value by about an order of magnitude. The main idea here is to show the accomplishment of setting up of an easy system (ISTB) to measure reduced beam brightness of an ion source, and potentially use it for low energy (1–30 keV) implantation and materials modification studies.

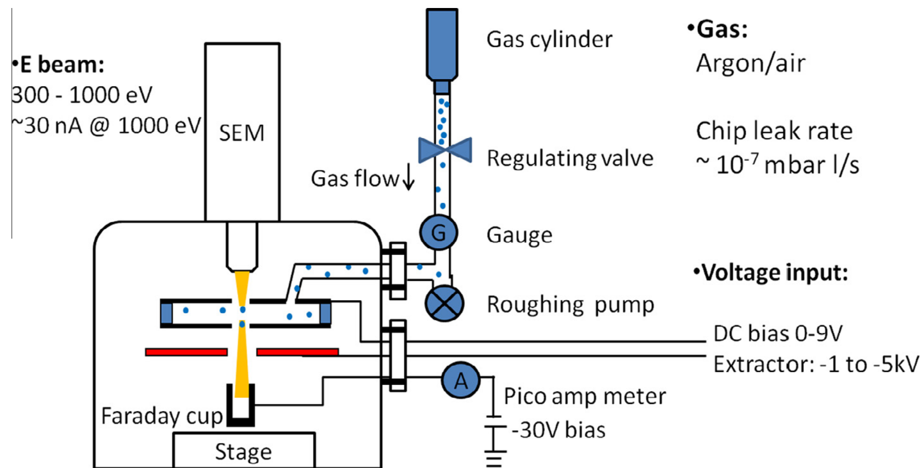

Fig. 5. Schematic of the experimental electron impact gas ion source test setup inside a Schottky emission SEM (Philips XL30) system in NUS.

3.2. Ion beam current measurement of the electron impact gas ion source

On the other hand, the extracted ion currents from the electron impact gas ion source using air and argon were studied as functions of the inlet pressure, the double aperture bias voltage and the extraction voltage, using a 1 keV primary electron beam.

Air with varying pressure from 1 mbar to 1 bar (measured using Varian FRG-702 vacuum Pirani gauge, after the regulating valve as shown in Fig. 5) was admitted into the gas chamber, and later ionized by the impact of 1 keV injection electron beam (~4 nA). The ionized beam is then extracted with an extraction voltage of −1250 V. Fig. 6 describes the measured ion beam current as a function of inlet pressure (Fig. 6a) and bias across the double aperture (Fig. 6b) for air. The error in the measurement is mainly due to the current integrator's measurement accuracy.

On the other hand argon gas with varying pressure from 1 mbar to ~1.6 bar (measured using dial vacuum gauge) was ionized in the gas chamber. The output ion beam current from the same double aperture was measured as a function of the gas inlet pressure and the extraction voltage (Fig. 7a and b, respectively). Here 1 keV injection electron beam (~26 nA) was used to ionize the Ar gas. The ions generated in this electron gas impact are mainly Ar^+ (about 89%) and the rest are Ar^{n+} (n = 2–4) [16].

Generally, the ion beam current increases with the gas inlet pressure, and should reach a maximum at certain optimal gas inlet pressure, at which point collisions between the ions and gas molecules become dominant, resulting in lower output current. The optimum gas pressure in the double aperture is expected where the gas molecule's mean free path λ is roughly the electron impact path length (see Fig. 2) [13]. The argon molecule's mean free path λ is given by $\lambda = kT(\sqrt{2}\pi PD^2)$, where k is the Boltzmann constant, T = 293 K, P the gas pressure and D = 0.369 nm the effective molecular diameter [17]. With an electron impact path length of around 2.2 μm (2 μm Si_3N_4 and 200 nm Ti spacer), the optimum argon gas inlet pressure is about 30 mbar. Meanwhile during the experiment the actual spacing between the double aperture is expected to get widened due to the deformation caused by the vacuum of the SEM. The spacing may increase to 1–2 μm from 200 nm, as observed by Jun et al. [18]. This deformation will effectively shift the optimal gas inlet pressure to a lower value, without changing the total ion beam current. But on the other hand this deformation will lead to an increased double aperture bias in order to obtain an optimal ion output current, and thereby increases the energy spread of the ion beam (as discussed in Section 2.2).

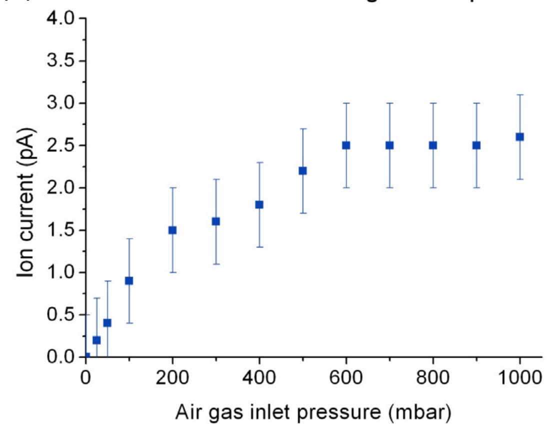

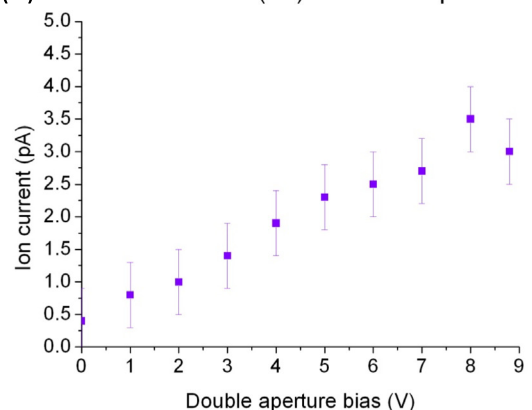

Fig. 6. The ion beam current measured with air, as a function of (a) gas inlet pressure, with a constant 8.8 V double aperture bias, and (b) double aperture bias voltage, with a constant gas inlet pressure of 1 bar. The major source of error in the measurement is the current integrator's accuracy.

It was observed that the ion current kept increasing with the air/argon gas inlet pressure (Figs. 6a and 7a, respectively). As the gas pressure was measured far away from the double aperture there is a large pressure drop between gauge and the double aperture. This was confirmed by the fact that the ion beam current did

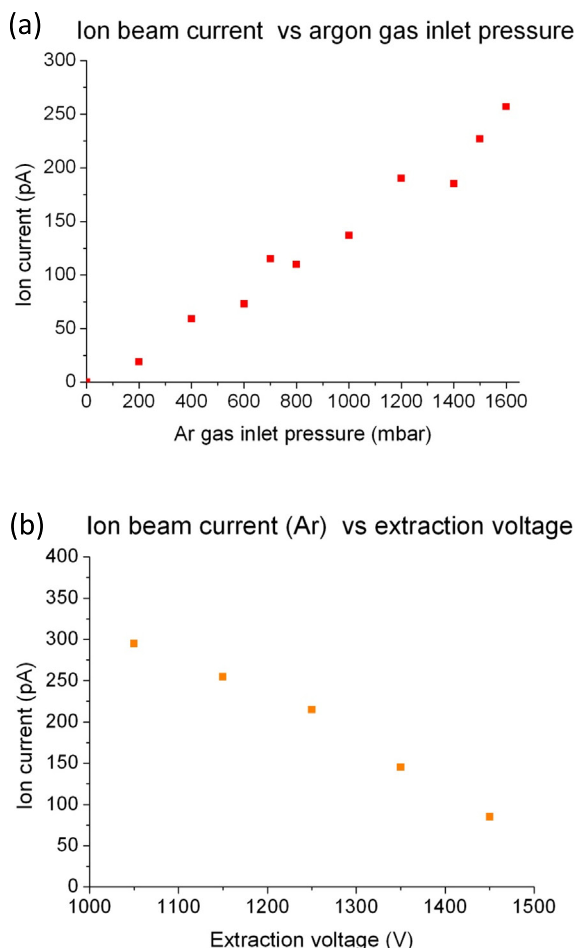

Fig. 7. The ion beam current measured with argon gas, as a function of (a) gas inlet pressure, with constant extraction voltage of −1250 V, and (b) variable extraction voltage, with constant gas inlet pressure of 800 mbar. The double aperture bias voltage was 8.8 V, with the injection electron beam of 1 keV.

not drop due to multiple collisions in the chip, for both air and Ar even for a maximum pressure of 1.0 bar and 1.6 bar, respectively. Any excess gas inlet pressure above 1.6 bar strongly influences the SEM chamber pressure, and thereby affecting the performance of electron column. In the next stage of our experiment, we plan to use a smaller-sized double aperture to reduce the gas leak rate through it. This will help to equalize the pressure along the gas feed channel.

With increasing double aperture bias voltage, the ion beam current (for air) is observed to increase (Fig. 6b). This is ascribed to the influence of a stronger electric field that facilitates ions from leaving the ionization chamber. However, this will also increase the energy spread of the ion beam, due to the fact that as the ions generated inside the gas chamber will have different initial energy depending on their ionization positions. This energy spread will be examined together with the focusing lens optics to reduce the chromatic aberration of the final ion beam size, in future experiments.

The ion beam current (for Ar) decreases with the extraction voltage (Fig. 7b) due to the fact that any extraction voltage higher than the injection electron beam acceleration voltage will start to distort the electron beam optics during operation. Another effect of the extraction voltage on the ion beam is its beam half divergence. When the extraction voltage is too high, the focal length of the extractor will be short and the ion beam will be more divergent, which corresponds to lower ion source brightness. Follow up experiments are required to establish the source brightness as a function of extraction voltage.

A fraction of extracted ions passing through the double aperture is likely to collide with the bottom chip membrane (as shown in Fig. 3). But it is not expected to affect the lifetime of the ion source, due to the following considerations:

1. The thermal energy of gas molecules at room temperature is only about 0.04 eV, corresponding to the maximum lateral kinetic energy. The chip bias voltage and extraction field assist to extract most of the ions through the double aperture. Only ions generated near the edge would have chance to collide with the bottom chip membrane. Focusing the electron beam in the center of the double aperture will improve the ion beam brightness and greatly reduce any ion collision with the bottom membrane.
2. Additionally, in future experiments, both sides of the chips' Si_3N_4 membranes will have a metal alloy layer coating (e.g. 10–100 nm Cr + Au). This coating is primarily used for biasing the chip, and is also used to conduct away stray ions, and electrons (which are deflected-back by the extractor). Thus ions having energy of up to 9 eV, would only penetrate less than 1 nm in the top Au layer of the Si_3N_4 membrane. SRIM simulation [19] predicts that there is practically no sputtering by these ions of the Au layer. Therefore ion sputtering is not likely to damage the aperture membrane and has insignificant influence on the ion source lifetime.

The ion beam current collected from a 1.5 μm diameter ion source aperture with Ar gas is about 300 pA with a beam energy of only 30 eV. Whereas in the existing PBW beam line at CIBA, NUS [20] with RF ion source, the 2 MeV H^+ beam current directly after the object slits (30 μm × 30 μm) is measured to be about 400 pA. The areal ion current density of the electron impact gas ion source is about 380 times higher than that of the RF ion source. The double aperture size can be further reduced to a diameter of about 100 nm. With the same primary electron current focused into this smaller double aperture, the ion source can provide an aerial current density up to 5 orders of magnitude higher than the existing RF ion source in CIBA.

4. Outlook and conclusion

We have established an ISTB, which is capable of integrating different ion sources (currently with RF ion source) and other essential components for the production and transport of high energy ion beams of different species. Initial measured B_r (~1.6 pA/μm^2 mrad^2 MeV), at large half divergence (1 mrad), of the present RF ion source is comparable with other similar systems measured at much lower half divergences (~0.1 mrad). Thus there is scope to improve the brightness through optimization of the ion source parameters, and reducing the half divergence in the present ISTB set-up. Meanwhile this ISTB will also serve to integrate and test any futuristic high brightness ion sources, to form a part of a compact proton beam writing system which will be designed to reach 200 kV, capable of writing sub-10 nm structures.

Parallel to this a miniaturized ion source chamber for electron impact gas ion source has been successfully tested inside a field emission SEM. With argon gas supplied, a beam current of 300 pA was collected from a 1.5 μm diameter double aperture. The ion source reduced brightness will be experimentally examined. The effects of electron beam energy and extraction voltage on B_r will be examined and more gas species will be tested (for example, helium, nitrogen and hydrogen). The theoretically calculated ion source reduced brightness for Ar^+ is about 10^7 pA/μm^2 mrad^2 MeV [13]. With an ion source B_r of the same

order for protons, it is expected to focus a 200 keV beam to sub-10 nm beam spot size with a beam current of about 10 pA on target. This PBW system is expected to be comparable to an Electron Beam Lithography (EBL) [21] system, with the advantage of fabricating high aspect ratio nanostructures with minimal proximity effects.

Acknowledgement

The authors would like to thank Professor P. Kruit and Associate Professor C.W. Hagen from Delft for discussions and inspiration. The authors also would like to acknowledge the financial support by U.S. Air Force, Japan office.

References

[1] J.A. van Kan, A.A. Bettiol, F. Watt, Nano Lett. 6 (2006) 579.
[2] F. Watt, M.B.H. Breese, A.A. Bettiol, J.A. van Kan, Mater. Today 10 (2007) 20.
[3] Y. Yao, M.W. van Mourik, P. Santhana Raman, J.A. van Kan, Nucl. Instrum. Methods Phys. Res. B 306 (2013) 265.
[4] Japanese governments' Nanotechnology Business Creation Initiative (NBCI) Roadmap 2010.
[5] Y. Yao, J.A. van Kan, Nucl. Instr. Meth. B 348 (2015) 203, http://dx.doi.org/10.1016/j.nimb.2014.12.066.
[6] Y. Yao, P. Santhana Raman, J.A. van Kan, Microsyst. Technol. 20 (2014) 2065.
[7] C.D. Moak, H. Reese, W.M. Good, Nucleonics 9 (1951) 18.
[8] R.R. Szymanski, D.N. Jamieson, Nucl. Instrum. Methods Phys. B. 130 (1997) 80.
[9] I. Kiss, E. Koltay, P.B. Pauspertl, Rev. Phys. Appl. (Paris) 12 (1977) 1481.
[10] V.I. Miroshnichenko, S.N. Mordik, V.V. Olshansky, K.N. Stepanov, V.E. Storizhko, B. Sulkio-Cleff, V. Voznyy, Nucl. Instrum. Methods Phys. B 201 (2003) 630.
[11] S.N. Mordyk, V.I. Voznyy, V.I. Miroshnichenko, A.G. Ponomarev, V.E. Storizhko, B.S. Cleff, Rev. Sci. Instrum. 75 (2004) 1922.
[12] N.S. Smith, W.P. Skoczylas, S.M. Kellogg, D.E. Kinion, P.P. Tesch, O. Sutherland, A. Aanesland, R.W. Boswell, J. Vac. Sci. Technol. B 24 (2006) 2902.
[13] D. Jun, P. Kruit, J. Vac. Sci. Technol. B 29 (2011) 6.
[14] LORENTZ 2D EM (Version 8.0) (Computer software), available from <http://www.integratedsoft.com>, 2009.
[15] D. Dahl, Int. J. Mass Spectrom. 200 (2000) 3.
[16] H.C. Straub, P. Renault, B.G. Lindsay, K.A. Smith, R.F. Stebbings, Phys. Rev. A 52 (1995) 1115.
[17] E.L. Cussler, Diffusion Mass Transfer in Fluid Systems, third ed., Cambridge University Press, New York, 2009, p. 120.
[18] D.S. Jun, V.G. Kutchoukov, C.T.H. Heerkens, P. Kruit, Microelectron. Eng. 97 (2012) 134.
[19] J.F. Ziegler, J.P. Biersack, U. Littmark, The Stopping and Range of Ions in Solids, Pergamon, New York, 1985 (Chapter 8), available: <http://www.srim.org>.
[20] J.A. van Kan, P. Malar, Armin Baysic de Vera, Rev. Sci. Instrum. 83 (2012) 02B902.
[21] M. Yan, S. Choi, K.R.V. Subramanian, I. Adesida, J. Vac. Sci. Technol. B 26 (2008) 2306.